Ensemble distribution for immiscible two-phase flow in porous media

Isha Savani,[1,*] Dick Bedeaux,[2,†] Signe Kjelstrup,[2,‡] Morten Vassvik,[1,§] Santanu Sinha,[3,‖] and Alex Hansen[1,¶]

[1]*Department of Physics, Norwegian University of Science and Technology, NTNU, N-7491 Trondheim, Norway*

[2]*Department of Chemistry, Norwegian University of Science and Technology, NTNU, N-7491 Trondheim, Norway*

[3]*Beijing Computational Science Research Center, 10 East Xibeiwang Road, Haidian District, Beijing 100193, China*

(Received 8 June 2016; published 27 February 2017)

We construct an ensemble distribution to describe steady immiscible two-phase flow of two incompressible fluids in a porous medium. The system is found to be ergodic. The distribution is used to compute macroscopic flow parameters. In particular, we find an expression for the overall mobility of the system from the ensemble distribution. The entropy production at the scale of the porous medium is shown to give the expected product of the average flow and its driving force, obtained from a black-box description. We test numerically some of the central theoretical results.

DOI: 10.1103/PhysRevE.95.023116

I. INTRODUCTION

Multiphase flow in porous media poses interesting problems to engineers and scientists in diverse fields [1]. Understanding the nature of multiphase flow is relevant to understand the flow of particles in bifurcating blood vessels, or to categorizing liquid transportation through cellulose. Other interesting areas concern spreading pollutants in soil, and the flow of hydrocarbons and water in oil reservoirs.

It is apparent from this wide range of applications of porous flow that the length scale of relevant processes can range from a few nanometers to several kilometers. In geological transport processes such as aquifers and oil reservoirs this fact is especially important, as the processes that occur at the pore scale (micron scale) remain important in attempting to understand the processes at the reservoir scale (kilometer scale).

When two immiscible fluids flow simultaneously in a rigid porous medium, the state-of-the-art description is given by the relative permeability equations, which are considered to be the effective medium equations. The relative permeability approach views each fluid as moving in a pore space that is constrained by the other fluid. Hence, each fluid will experience a lowered effective permeability since it experiences a diminished pore space in which to move. The ratios between the effective permeabilities of each fluid and the single-fluid permeability of the porous medium are the relative permeabilities. The relative permeabilities are thought only to depend on the fluid saturations (which are the volumes of each fluid relative to the pore volume). In addition to the relative permeabilities, a capillary pressure field that models the interfacial tension between the two fluids is introduced [2].

The concept of relative permeability is simple. However, different laboratory methods, e.g., the Penn State or the Hassler method [3], yield different results for the measurement of relative permeability. This signals that the relative permeability equations do not offer a complete description of the problem. These weaknesses have been known for a long time and it is not controversial to state that the relative permeability approach should and probably will be replaced by a better framework. Several attempts have been made to replace this framework; see, e.g., Refs. [4–24].

Techniques for recording and reconstructing the pore structure of porous media have developed tremendously over the last years [25]. It is now possible to render detailed maps of the structure of porous media at the subpore level.

Numerical techniques to calculate the flow properties have also developed and branched out over the years. There are several approaches. Bryant and Blunt [26] were the first to calculate relative permeabilities from a detailed network model. Aker *et al.* [27,28] developed a network model which was extended to include film flow by Tørå *et al.* [29]. The model is today being combined with a Monte Carlo technique [30] to speed up the calculations considerably. A recent review summarizes the status of this class of models; see Ref. [31]. A very different approach is the lattice Boltzmann method [32,33]; see also Refs. [34,35]. Whereas the network models are ideal for large networks without detailed knowledge of the precise shape of each pore, the lattice Boltzmann method has the opposite strength. It goes well with the detailed pore spaces that are now being reconstructed, but is less useful in large networks. Other methods than the lattice Boltzmann one, which resolve the flow at the pore level, are, e.g., smoothed particle hydrodynamics [36–38] and density functional hydrodynamics [39].

The goal of any theory of immiscible two-phase flow in porous media must be to bind together the physics at the pore level with a description at scales where the porous medium may be seen as a continuum. We illustrate this viewpoint through the relative permeability equations that attempt to do exactly this:

$$\vec{v}_w = -\frac{K}{\mu_w} k_{r,w} \vec{\nabla} P_w \tag{1}$$

and

$$\vec{v}_n = -\frac{K}{\mu_n} k_{r,n} \vec{\nabla} P_n. \tag{2}$$

Here $\vec{v}_w$ and $\vec{v}_n$ are the Darcy velocities of the wetting and nonwetting fluids, μ_w and μ_n are the viscosities of the wetting

*Isha.Savani@gmail.com
†Dick.Bedeaux@chem.ntnu.no
‡Signe.Kjelstrup@ntnu.no
§Morten.Vassvik@ntnu.no
‖Santanu@csrc.ac.cn
¶Alex.Hansen@ntnu.no

and nonwetting fluids, K is the permeability of the porous medium, $k_{r,w}(s)$ and $k_{r,n}(s)$ are the relative permeabilities of the wetting and nonwetting fluids, and s is the nonwetting saturation. One distinguishes between the pressure in the wetting fluid, P_w, and that in the nonwetting fluid, P_n. They are related through the capillary pressure $P_c(s)$ by

$$P_n - P_w = P_c. \tag{3}$$

The relative permeabilities and the capillary pressure are assumed to be functions of the nonwetting fluid saturation s alone. These equations treat the porous medium as a continuum. There are three functions entering these three equations that are determined by the physics at the pore level: $k_{r,w}(s)$, $k_{r,n}(s)$, and $P_c(s)$.

An alternate recent theory [24] based on thermodynamics [40,41] proposes the relations

$$\frac{d\vec{v}}{ds} = \vec{v}_n - \vec{v}_w \tag{4}$$

and

$$s\frac{d\vec{v}_n}{ds} + (1-s)\frac{d\vec{v}_w}{ds} = 0, \tag{5}$$

where $\vec{v} = s\vec{v}_n + (1-s)\vec{v}_w$ is the saturation-weighted average Darcy velocity. The pore-level physics enters the picture through the constitutive equation $\vec{v} = \vec{v}(s, \vec{\nabla} P)$, where P is the pressure.

The functions $k_{r,w}(s)$, $k_{r,n}(s)$, and $P_c(s)$, or in the last case $\vec{v} = \vec{v}(s, \vec{\nabla} P)$ are macroscopic functions; they are defined at the continuum level. Other theories will have other macroscopic functions that connect the pore-level physics to the continuum level. Such functions are the results of the collective behavior of the fluids in vast numbers of pores. To be able to calculate the precise behavior of the fluids in a small number of pores as is done using the lattice Boltzmann method is not enough to determine fully the physics at large scales. This is well known in other fields such as statistical mechanics where long-range correlations that are generated by the short-range interactions between the microscopic components may dominate the behavior.

It is therefore tempting to develop a *statistical mechanics* for immiscible two-phase flow in porous media. The goal of statistical mechanics is precisely to bind the microscopic and the macroscopic worlds together, and it has been very successful in this in the past. We in this paper attempt to take the first steps in this direction.

In the 1950s through the 1960s, work was done on a statistical description of flow in porous media [42–45]. Since the late 1980s, a theory of two-phase flow using a thermodynamic approach has been developed and employed by Hassanizadeh and Gray [5,6,9,11]. More recently, Valavanides and Daras [22] employed tools from statistical mechanics to describe flow. Hansen and Ramstad [16] proposed to develop a thermodynamical description of immiscible two-phase flow in porous media based on the configurations of the fluid interfaces, an approach that is related to that of Valavanides and Daras.

In the spirit of Hansen and Ramstad [16], we aim to develop a statistical description of the flow of two immiscible fluids through a two-dimensional network by constructing a macroscopic description that applies to the ensemble-averaged behavior of all connected links. Sinha *et al.* [46] derived a statistical description of steady-state two-phase flow in a single capillary tube. They showed that the well-known Washburn equation could be derived from the entropy production in the tube. They verified that the system was ergodic and derived an analytical expression for the ensemble distribution. The ensemble distribution is the probability distribution of finding the center of mass of a bubble of the nonwetting liquid at a particular position in the tube. The ensemble distribution in the one-dimensional case was found to be inversely proportional to the velocity of the nonwetting bubble. Given that a slow bubble stays proportionally longer in a link, this velocity dependence is self-evident. This idea was developed further, by demonstrating in Ref. [30] that the probability for a given configuration of interfaces in a network, not just a one-dimensional one, is proportional to the inverse of the total flow through the network. This probability distribution was then used to form the basis for a Markov-chain Monte Carlo method for sampling configurations in a network model.

Whereas the *configurational probability distribution* that was derived by Savani *et al.* [30] gave the probability density for the interfaces between the fluids forming a given configuration in the *entire network,* we here construct an *ensemble distribution* for the *individual links.* That is, we derive the joint probability density for any link in the network to have a given saturation, that the nonwetting fluid it contains will have its center of mass at a given position and that its radius will have a given value.

We consider here for concreteness a network of pores each characterized by a length and a radius. We define flow velocity and saturations for each link and set up the joint statistical distribution between these and the radius distribution. We assume that the porous medium—the network of pores—is homogeneous. This implies that if there are two statistically similar networks, the combined system will have the same properties as the separate systems.

The paper is organized as follows. In Sec. II we describe the porous medium model we use for the theoretical derivations. We use a biperiodic square lattice where the links model the pores. This simplifies the theoretical discussion while retaining the complexity of the flow. Section III introduces the ensemble distribution that provides the joint probability distribution for pore radius, pore saturation, and the position of bubbles in the pores. The first of these variables characterizes the porous medium whereas the other two characterize the flow. We go on to demonstrate that the ensemble distribution is inversely proportional to the volume flow through the links. We also demonstrate that the system is ergodic. Section IV connects the ensemble distribution with different macroscopic quantities, namely, the fractional volume flow, the saturation, the pressure difference, and the entropy production. In Sec. V we test numerically some of the central results of the previous sections. Our conclusions are given in Sec. VI.

II. DEFINING THE VARIABLES CHARACTERIZING THE FLOW AND THE POROUS MEDIUM

In the same way as Bakke and Øren [47,48] extracted a network from the pore space of a porous medium, we replace

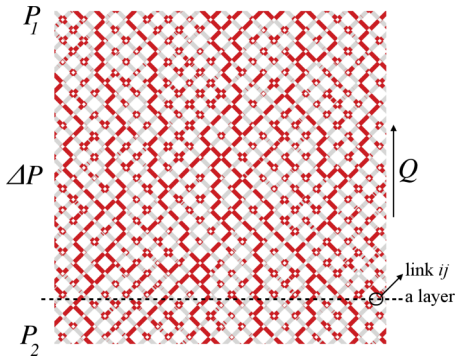

FIG. 1. Our network model, which is described in detail in the Appendix, consists of a square lattice oriented at 45° with respect to the vertical direction; see arrow. The network is periodic in both the vertical and horizontal directions. Hence, fluids that leave the network along the upper border reappear at the bottom border, and fluids that leave along the left border enter at the right border and vice versa. The links are filled with an immiscible mixture of wetting (white) and nonwetting (red) fluids. A pressure difference $\Delta P = P_1 - P_2$ between the upper and lower borders drives the flow Q in the vertical direction. The nonwetting fluids form channels that span the network once the flow has reached steady state as shown in the figure. Steady-state flow means that the average flow parameters such as Q fluctuate around well-defined constant average values, whereas, at the level of the links, the interfaces between the immiscible fluids move,resulting in fluid clusters constantly merging and breaking up.

the original porous medium by a network representing its pore space. All our variables aredefined with reference to the links in this network.

In this paper, however, we go one step further and consider a lattice in the form of a square grid. This is of course a considerable and unrealistic simplification compared to the topology of a real pore network. However, as the goal of this work is *not* to consider a given structure but to develop a *general theory,* it is convenient to use the square network. It simplifies the discussion while retaining the important subtleties. The square lattice is periodic in both directions. We orient it so that the main axes form 45° with the average flow direction; see Fig. 1. There are $L \times L$ distinct links in the lattice. This means that there are L distinct layers of links; see Fig. 1. For a square lattice, the total number of nodes is then $L^2/2$ and a link between two neighboring nodes i and j is denoted by ij where $i, j \in [0, L^2/2]$.

We assume that all links in the network have the same length l. The radius $r_{0,ij}$ varies from link to link and is drawn from a spatially uncorrelated distribution $f_r(r_{0,ij})$.

A volume flow Q across the network in the vertical direction generates a pressure difference across one layer $\Delta P/L$ depending on s in the opposite direction; see Fig. 1.

We define the nonwetting saturation s_{ij} in link ij as

$$s_{ij} \equiv \frac{v_{n,ij}}{v_{ij}}, \tag{6}$$

where $v_{n,ij}$ refers to the volume of nonwetting fluid in the link and v_{ij} is the total volume of the link.

We assume that the wetting fluid does not wet the pores completely so that it does not form films. The nonwetting fluid will form bubbles that fill the cross-sectional area of the links. We characterize their motion through the time derivative of one position variable $x_{b,ij}$ which signifies, e.g., the position of their center of mass measured along the link of length l; hence, $0 \leqslant x_{b,ij} \leqslant l$.

We consider steady-state flow [49]. Experimentally, this is attained when the two immiscible fluids are injected simultaneously into the porous medium with all control parameters kept constant, and all measured macroscopic quantities fluctuate around well-defined and constant averages. In our square lattice, the steady state is attained when the fluids are allowed to circulate long enough in the biperiodic network. The steady state does *not* imply that the interfaces at the pore level are static. Rather, ΔP may be so high that all interfaces move and the system would still be in the steady state.

III. ENSEMBLE DISTRIBUTION

At a given moment in time, there is a certain configuration of the two fluids in the network. The ensemble distribution is derived from this snapshot and is considered to be a time-independent probability distribution of the two fluids over the ensemble of links since the flow appears under steady-state conditions. The exact nature of the ensemble distribution is still unknown, however. The aim of this work is to derive some of its properties. Such knowledge will enable the integration across the network for determining various properties of interest. For instance, we are interested in the average pressure difference and the fractional volume flow of the wetting and the nonwetting fluids when the total volume flow Q and s are imposed. In particular we are interested in the total volume flows of each of the single fluids. Thermodynamics on the macroscopic level has recently been used to relate these quantities [24]; however, this approach is entirely macroscopic. Using an ensemble distribution, we can build a bridge between the properties of a single link and the overall performance of the network. We aim to develop a new method that can solve the up-scaling problem in the context of immiscible multiphase flow in porous media.

The ensemble distribution we develop in the following is at the *indivual link level.* That is, we pick a link in the network at random. What is the joint probability density that this link has a given radius, saturation, and center-of-mass position of the nonwetting bubbles in it?

As was stated in the introduction, this is different from the configurational probability distribution; that is, the probability density for the interfaces between the two fluids takes on a given configuration in the network, which was derived by Savani *et al.* [30] and used to construct a Markov-chain Monte Carlo algorithm for sampling configurations in network models.

A. The one-dimensional distribution

Working towards the goal to determine the ensemble distribution beyond one dimension, we start by rederiving the distribution for a link [30,46]. The time average of any function

$g = g(x_b)$ is $\overline{g}$, where

$$\overline{g} = \frac{1}{\tau}\int_0^\tau dt g(x_b(t)) = \int_0^l dx_b \frac{g(x_b)}{\tau dx_b/dt} = \int_0^l dx_b \Pi(x_b) g(x_b). \quad (7)$$

This allows us to extract the *ensemble distribution*

$$\Pi(x_b) = \frac{1}{\tau}\frac{1}{dx_b/dt} = \frac{1}{l}\frac{\langle q\rangle}{q(x_b)} \quad \text{for} \quad 0 < x_b < l, \quad (8)$$

where $\tau = \pi {r_0}^2 l/\langle q\rangle$ is the average time the bubble takes to move from one end of the link to the other end, and $\langle q\rangle$ is the ensemble average volume flow. $\Pi(x_b)$ is the ensemble distribution since it gives the probability density for x_b. This is a general result that is valid even if the velocity dx_b/dt is not constant. For a detailed discussion see Ref. [30]. By definition we have that

$$\int_0^l dx_b \Pi(x_b) g(x_b) = \langle g\rangle. \quad (9)$$

Hence, combining this expression with Eq. (7) gives

$$\overline{g} = \langle g\rangle, \quad (10)$$

demonstrating that the system by construction is ergodic [46].

B. Ensemble distribution in higher dimensions

In higher dimensions, at any instance, the state of a link can be characterized by the center-of-mass position of the bubbles in it, $x_{b,ij}$, the saturation s_{ij}, and the radius $r_{0,ij}$ of the link. In the course of time, a single link will see the passage of many bubbles with different sizes. One may calculate the time average of q_{ij} for each individual link.

A subsequent average over the radii of the links returns the average volume flow $\langle q\rangle$ in the links. A fast bubble will spend proportionally less time in a given link than a slow bubble. This is true whether the link is part of a one-dimensional or a multidimensional network. This suggests that also in the multidimensional case, the ensemble distribution, $\Pi(x_{b,ij},s_{ij},r_{0,ij})$, will be inversely proportional to the volume flow $|q_{ij}(x_{b,ij},s_{ij},r_{0,ij})|$. By the same argument that led to Eq. (10) and, hence, ergodicity, the multidimensional system must be ergodic.

A general form of the ensemble distribution is

$$\Pi(x_{b,ij},s_{ij},r_{0,ij}) = \frac{\langle|q|\rangle}{|q_{ij}(x_{b,ij},s_{ij},r_{0,ij})|} f(x_{b,ij},s_{ij},r_{0,ij}) \quad \text{for } 0 < x_{b,ij} < l \text{ and } 0 < s_{ij} < 1, \quad (11)$$

where $f(x_{b,ij},s_{ij},r_{0,ij})$ is assumed to be normalized. The distribution $f(x_{b,ij},s_{ij},r_{0,ij})$ may, in principle, depend on the volume flow $q_{ij}(x_{b,ij},s_{ij},r_{0,ij})$.

IV. FROM ENSEMBLE DISTRIBUTION TO MACROSCOPIC QUANTITIES

The aim of this section is to calculate the fractional volume flow of the nonwetting fluid, the saturation, the pressure drop, and the entropy production, all macroscopic variables, from the ensemble distribution.

A. Average absolute volume and fractional volume flows

The average absolute volume flow is given by

$$\langle|q|\rangle = \int_0^\infty dr_{0,ij}\int_0^1 ds_{ij}\int_0^l dx_{b,ij}\Pi(x_{b,ij},s_{ij},r_{0,ij})| \times q_{ij}(x_{b,ij},s_{ij},r_{0,ij})|. \quad (12)$$

This form can be verified by introducing the general ensemble distribution in Eq. (11), and using that f is normalized. It turns out that the form of the general ensemble distribution in Eq. (11) is sufficient to obtain this result.

The total absolute volume flow in the direction of the pressure difference through one layer (see Fig. 1) is equal to

$$|Q'| \equiv \sum_{ij} |q_{ij}(x_{b,ij},s_{ij},r_{0,ij})|, \quad (13)$$

where the summation is over all the links ij in that particular layer.

The total absolute volume flow through the cross section or through each layer is the same for incompressible fluids; hence, $|Q'| = |Q|$. The average is equal to

$$\langle|Q|\rangle = L\langle|q|\rangle, \quad (14)$$

where L is the number of links in a layer. The last equality expresses the fact that the links in a layer form an ensemble of links with the ensemble distribution given in Eq. (11).

We proceed to calculate the absolute fractional flow through the system. The average of the total absolute volume flow of the nonwetting fluid in the direction of the overall pressure difference is equal to

$$\langle|Q_n|\rangle \equiv L\langle|q_{n,ij}(x_{b,ij},s_{ij},r_{0,ij})|\rangle = L\langle s_{ij}|q_{ij}(x_{b,ij},s_{ij},r_{0,ij})|\rangle. \quad (15)$$

With the help of the ensemble distribution, the absolute flow of the nonwetting fluid equals

$$\begin{aligned}\langle|Q_n|\rangle &= L\int_0^\infty dr_{0,ij}\int_0^1 ds_{ij}\int_0^l dx_{b,ij} \times\Pi(x_{b,ij},s_{ij},r_{0,ij})s_{ij}|q_{ij}(x_{b,ij},s_{ij},r_{0,ij})| \\ &= L\langle|q|\rangle\int_0^\infty dr_{0,ij}\int_0^1 ds_{ij}\int_0^l dx_{b,ij} \times s_{ij} f(x_{b,ij},s_{ij},r_{0,ij}) \\ &= L\langle|q|\rangle\langle s\rangle. \end{aligned} \quad (16)$$

The nonwetting fraction of the absolute volume flow is then equal to

$$F \equiv \frac{\langle|Q_n|\rangle}{\langle|Q|\rangle} = \int_0^\infty dr_{0,ij}\int_0^1 ds_{ij}\int_0^l dx_{b,ij} s_{ij} f(x_{b,ij},s_{ij},r_{0,ij}) = \langle s\rangle. \quad (17)$$

The fraction of the total absolute nonwetting volume flow is therefore equal to the ensemble average of the degree of saturation. Again, the form of the general ensemble distribution equation, Eq. (11), is sufficient to obtain this result. The relation can be tested numerically and experimentally with information of the distributions. We show that it is obeyed for a particular network in the end of the paper.

Equation (17) is at a first glance surprising, but it should be remembered that the average saturation is *per link* and not per volume. We test Eq. (17) in Fig. 7.

B. Average saturation

The volume average of the saturation of the links in any layer is given by

$$s \equiv \frac{V_n}{V} = \frac{\sum_j v_{ij}s_{ij}}{\sum_j v_{ij}} = \frac{\int_0^\infty dr_{0,ij}\int_0^1 ds_{ij}\int_0^l dx_{b,ij}\,v_{ij}s_{ij}\Pi(x_{b,ij},s_{ij},r_{0,ij})}{\int_0^\infty dr_{0,ij}\int_0^1 ds_{ij}\int_0^l dx_{b,ij}\,v_{ij}\Pi(x_{b,ij},s_{ij},r_{0,ij})} = \frac{\langle vs\rangle}{\langle v\rangle}. \tag{18}$$

In the one-dimensional sequence of links, all the links have the same volume $v_{ij} = \pi l r_{0,ij}^2$, so that $\langle s\rangle = s$. This implies that the fraction of the total absolute nonwetting volume flow is given by $F = s$. This is generally not the case in multidimensional systems, except when there are no capillary forces.

An interesting observation is that when the distribution of the saturation and the radius are not correlated, it follows that

$$f(s_{ij},r_{0,ij}) \equiv \int_0^l dx_{b,ij}\,f(x_{b,ij},s_{ij},r_{0,ij}) = f_s(s_{ij})f_r(r_{0,ij}). \tag{19}$$

This implies that

$$F = \langle s\rangle = s. \tag{20}$$

At high capillary numbers, one has that $F = s$ since the capillary forces play no role. This implies Eq. (20) is valid in the high-capillary-number regime. In Fig. 8 we plot F vs s for Ca $= 0.01$ and 0.1. For the lower capillary number, we see a nontrivial dependence of F on s. However, for the larger capillary number, we see F being close to s signaling that s_{ij} and r_{ij} decorrelate and Eq. (20) ensues.

C. Average pressure difference

In experiments or simulations in which the volume flow is controlled, the pressure difference cannot be fixed. The fluctuating driving force follows from Eq. (A2):

$$\Delta p_{ij}(x_{b,ij},s_{ij},r_{0,ij}) - p_{c,ij}(x_{b,ij},s_{ij},r_{0,ij}) = -\frac{8\mu_{av,ij}(s_{ij})}{\pi r_{0,ij}^4}q_{ij}(x_{b,ij},s_{ij},r_{0,ij}), \tag{21}$$

where $p_{c,ij}(x_{b,ij},s_{ij},r_{0,ij})$ is the capillary pressure drop due to interfaces in the link and $\Delta p(x_{b,ij},s_{ij},r_{0,ij})$ is the pressure drop across the link and $\mu_{av,ij} = s_{ij}\mu_n + (1-s_{ij})\mu_w$ is the volume-weighted average viscosity. Using the ensemble distribution, the absolute average driving force is given by

$$\langle|\Delta p - p_{c,ij}|\rangle = \frac{8}{\pi}\int_0^\infty dr_{0,ij}\int_0^1 ds_{ij}\int_0^l dx_{b,ij} \times \Pi(x_{b,ij},s_{ij},r_{0,ij})\frac{\mu_{av,ij}(s_{ij})}{r_{0,ij}^4}| \times q_{ij}(x_{b,ij},s_{ij},r_{0,ij})|. \tag{22}$$

By introducing Eq, (11) for the ensemble distribution, we obtain

$$\langle|\Delta p - p_{c,ij}|\rangle = \frac{8}{\pi}\langle|q|\rangle\int_0^1 ds_{ij}\int_0^\infty dr_{0,ij} \times \frac{\mu_{av,ij}(s_{ij})}{r_{0,ij}^4}f(s_{ij},r_{0,ij}). \tag{23}$$

Using this expression, one can find the overall mobility M of the fluids in the network,

$$\mathrm{M} = \frac{\langle|q|\rangle}{\langle|\Delta p - p_{c,ij}|\rangle} = \frac{\pi}{8}\left[\int_0^1 ds_{ij}\int_0^\infty dr_{0,ij}\frac{\mu_{av,ij}(s_{ij})}{r_{0,ij}^4}f(s_{ij},r_{0,ij})\right]^{-1}, \tag{24}$$

which corresponds to Darcy's law for the system.

D. The entropy production

In nonequilibrium thermodynamics, the second law is formulated in terms of the entropy production in the system [40,41]. The entropy production quantifies the energy dissipated in the form of heat in the surroundings. In the present case, this amounts to the viscous dissipation. According to the second law, the dissipation is always positive. The expression for the entropy production in terms of the ensemble distribution must obey this condition at a local level, i.e., at the scale of a single link. For the whole system, we can find the average entropy production using Eq. (11):

$$\begin{aligned} T\left\langle\frac{dS_{\mathrm{irr}}}{dt}\right\rangle &= -\int_0^\infty dr_{0,ij}\int_0^1 ds_{ij}\int_0^l dx_{b,ij} \times \Pi(x_{b,ij},s_{ij},r_{0,ij})q_{ij}(x_{b,ij},s_{ij},r_{0,ij}) \times [\Delta p_{ij} - p_{c,ij}(x_{b,ij},s_{ij},r_{0,ij})] \\ &= \langle|q|\rangle\int_0^\infty dr_{0,ij}\int_0^1 ds_{ij}\int_0^l dx_{b,ij} \times f(x_{b,ij},s_{ij},r_{0,ij})|\Delta p_{ij} - p_{c,ij}(x_{b,ij},s_{ij},r_{0,ij})| \\ &= \langle|q|\rangle\langle|\Delta p - p_{c,ij}|\rangle. \end{aligned} \tag{25}$$

In the second equality we used that q_{ij} and $(\Delta p - p_{c,ij})$ have opposite signs in accordance with the second law of thermodynamics. We see that the local as well as the global entropy production have the correct bilinear form. This confirms that the ensemble distribution given in Eq. (11) is the correct choice.

V. NUMERICAL VERIFICATION

We test and develop numerically some of the main results of the previous sections using the network model described in the Appendix.

The network was initialized with a random configuration of bubbles for a desired saturation s. Measurements were started only after the system had reached steady state.

We used a spatially uncorrelated uniform distribution on the interval [0.1,0.4] mm for the radii. The length of the links

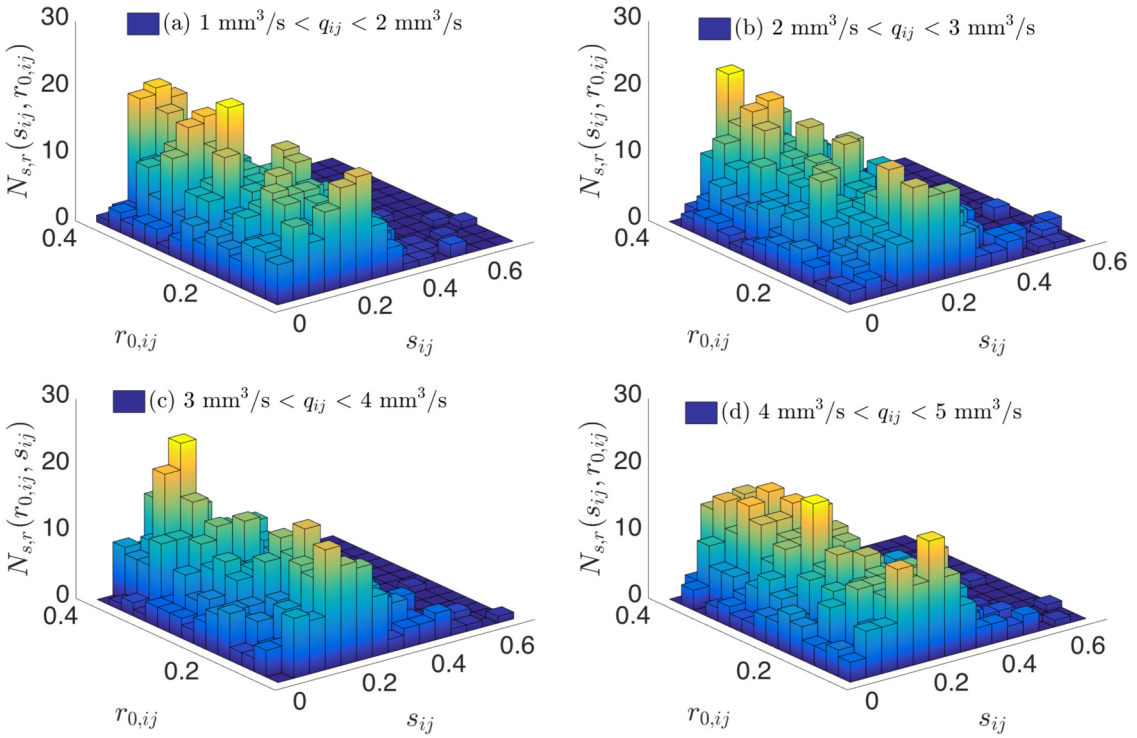

FIG. 2. Joint histogram $N_{s,r}$ for $r_{0,ij}$ and s_{ij} for the given ranges of q_{ij} for Ca = 0.01 and $s = 0.2$.

was 1 mm. The nonwetting and wetting model fluids were given the same viscosity, $\mu = 0.1$ Pa s. The surface tension γ between the fluids was set to 30 mN/m.

The simulations were performed for two different volume flows that were kept constant throughout the simulations, $Q = 26$ and $Q = 260\,\mathrm{mm}^3/\mathrm{s}$. They corresponded to a capillary number, defined as

$$\mathrm{Ca} \equiv \frac{Q\mu}{A\gamma}, \tag{26}$$

where A is defined as the cross section of the network given by $\sum_{ij} \pi r_{0,ij}^2$ where the sum runs over a layer. The capillary numbers were Ca = 0.01 and 0.1. The system size was $L \times L = 40 \times 40$ except in Figs. 4, 5, and 6, where also $L \times L = 20 \times 20$ was used. Results are averaged over ten samples for each series of measurements with different capillary number.

In Eq. (11) we give the general form of the configurational probability. In Fig. 2, we show histograms $N_{s,r}$ proportional to the joint probability distribution for s_{ij} and $r_{0,ij}$ when only those links which fall within a narrow range of volume flows are counted. That is, we record only those links for which (a) $1 < q_{ij} < 2$ mm^3/s, (b) $2 < q_{ij} < 3$ mm^3/s, (c) $3 < q_{ij} < 4$mm^3/s, and (d) $4 < q_{ij} < 5$ mm^3/s. The volume flows q_{ij} ranged roughly between -2.5 and 7.5 mm^3/s. If $f(x_{b,ij},s_{ij},r_{0,ij}) = f(s_{ij},r_{0,ij})$, i.e., if $x_{b,ij}$ was uncorrelated with s_{ij} and $r_{0,ij}$, then the histograms in the four figures should be identical. We see that, even though the features are similar, they are not. Hence, there is an $x_{b,ij}$ dependence in $f(x_{b,ij},s_{ij},r_{0,ij})$ for Ca = 0.01.

We may transform the distribution in Eq. (11) from a distribution in $x_{b,ij}$ to a distribution in $|q_{ij}|$:

$$\Pi_q(|q_{ij}|,s_{ij},r_{0,ij}) = \frac{\langle|q|\rangle}{|q_{ij}|} f(x_{b,ij}(|q_{ij}|,s_{ij},r_{0,ij}),s_{ij},r_{0,ij}) \times \left[\frac{\partial}{\partial|q_{ij}|}\right] x_{b,ij}(|q_{ij}|,s_{ij},r_{0,ij}). \tag{27}$$

We show in Fig. 3 the cloud of values measured in the system for Ca = 0.01 and $s = 0.5$. It is this cloud that Eq. (27) describes.

We show in Fig. 4 histograms N_q proportional to Π_q for Ca = 0.1 and for two different system sizes, $L \times L = 20 \times 20$ and $L \times L = 40 \times 40$. The volume flows Q have

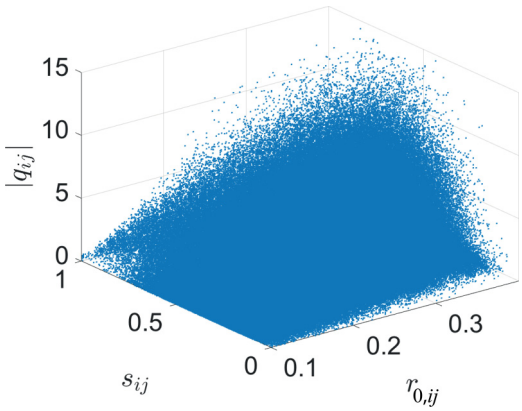

FIG. 3. A cloud plot of $|q_{ij}|$, s_{ij}, and $r_{0,ij}$ for Ca = 0.01 and $s = 0.5$.

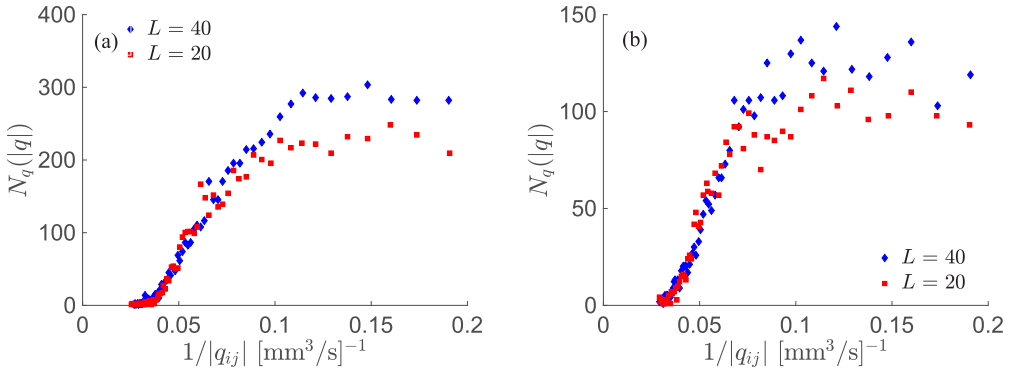

FIG. 4. Histogram $N_q(|q|)$ of volume flow in links when $0.4 < s_{ij} < 0.5$ and $0.2 < r_{0,ij} < 0.3$ mm for Ca $= 0.1$ and (a) $s = 0.3$ or (b) $s = 0.4$.

been adjusted so that the capillary numbers are the same for the two system sizes. Only those links with values of the other two parameters, s_{ij} and $r_{0,ij}$, within a truncated range have been recorded. In Figs. 5 and 6 we show the corresponding histograms for Ca $= 0.01$. The histograms for Ca $= 0.1$ show a gap for small values of $1/|q_{ij}|$, and for increasing values of $1/|q_{ij}|$ a somewhat linear region before an essentially flat region occurs. It is not possible from the results for the two system sizes to infer a clear trend that could make it possible to extrapolate the result to infinite system size. The corresponding histograms for the Ca $= 0.01$ case are in Figs. 5 and 6. They are qualitatively different from the histograms for Ca $= 0.1$, Fig. 4. There is still a gap for small values of $1/|q_{ij}|$, but from a smallest value, $1/|q_{0,ij}| = 1/|\max_{ij} q_{ij}|$, the histogram raises linearly. We also note that the $L = 40$ data give a straighter line than the $L = 20$ data. Since the volume flow Q is kept fixed, there is a largest possible link volume flow in the system: $\max_{ij} |q_{ij}| = |Q|$. This would occur if Q in its entirety passed through one link, a possibility that would be more and more likely the smaller the capillary number due to capillary blocking. Hence, for Ca $= 0.01$, $\Pi_q(|q_{ij}|)$ takes the form

$$\Pi_q(|q_{ij}|) = g(s_{ij},r_{0,ij})\left[\frac{1}{|q_{ij}|} - \frac{1}{|Q|}\right], \tag{28}$$

where

$$g(s_{ij},r_{0,ij}) = \langle |q| \rangle f(x_{b,ij}(|q_{ij}|,s_{ij},r_{0,ij}),s_{ij},r_{0,ij}) \left[\frac{\partial}{\partial |q_{ij}|}\right] \times x_{b,ij}(|q_{ij}|,s_{ij},r_{0,ij}). \tag{29}$$

The $|Q|$ dependence in Eq. (28) comes from the use of the constant-Q ensemble. If each run had been done with ΔP, the pressure drop across the network, kept constant, the $1/|Q|$ term may have vanished. It was shown by Batrouni *et al.* [50] that the choice of ensemble, constant Q or constant ΔP, had a profound influence on the high-current end of the current histogram in the random resistor network, a system that shares some similarity to the present one.

It should be noted that the immiscible two-phase-flow problem undergoes a phase transition when the saturation is tuned [51]. For the square lattice, they found the critical saturation to be $s_c = a + b \log_{10} \text{Ca}$, where $a = 0.8$ and $b = 0.063$. For Ca $= 0.01$, this places the critical point at around $s_c \approx 0.67$. In analogy with the random resistor network at the percolation threshold, we expect $\Pi_q(|q_{ij}|)$ to have a much more complex form than suggested in Eq. (29) [52,53], namely that of a multifractal. This has recently been suggested in connection with immiscible two-phase counterflow in porous media [54].

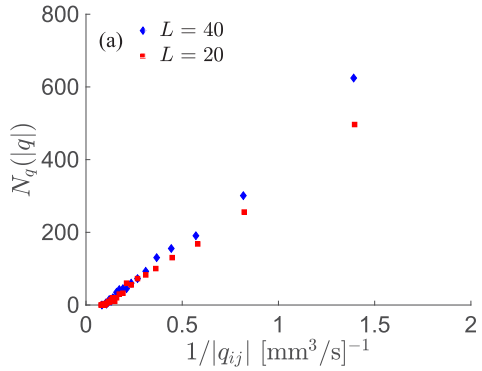

FIG. 5. Histogram $N_q(|q|)$ of volume flow in links when $0.3 < s_{ij} < 0.4$ and $0.2 < r_{0,ij} < 0.3$ mm for Ca $= 0.01$ and $s = 0.3$.

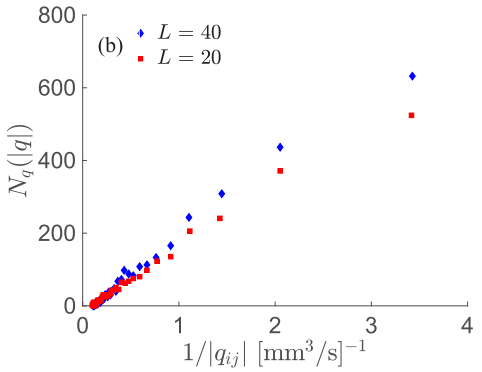

FIG. 6. Histogram $N_q(|q|)$ of volume flow in links when $0.4 < s_{ij} < 0.5$ and $0.2 < r_{0,ij} < 0.3$ mm for Ca $= 0.01$ and $s = 0.5$.

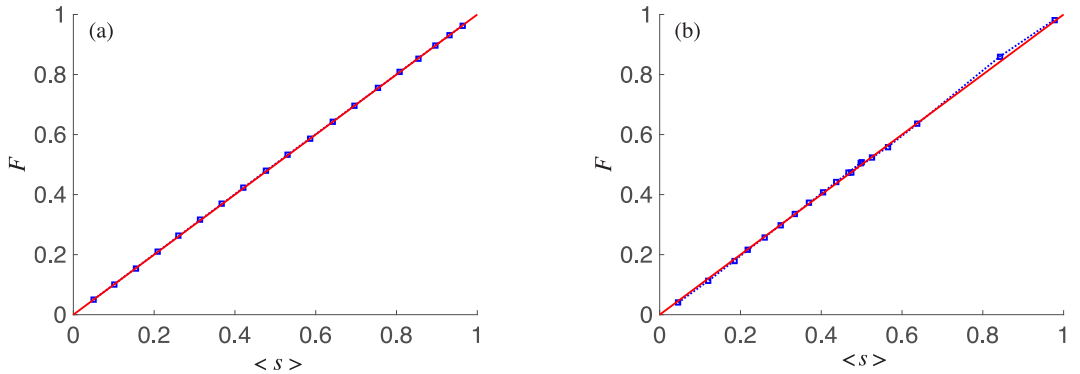

FIG. 7. The nonwetting fractional flow defined in Eq. (17) F vs the saturation averaged over the links, $\langle s \rangle$ for (a) Ca $= 0.1$ and (b) Ca $= 0.01$. According to this equation, we expect $F = \langle s \rangle$. This is also what we observe.

In Sec. IV it was shown that $F = \langle s \rangle$, Eq. (17), even if capillary forces are important. We demonstrate by calculation the validity of this relation in Fig. 7. In Fig. 8 we show F as a function of volume-weighted average of the saturation s. As expected, we see that F is a nontrivial function of s. However, for larger capillary numbers, F is closer to the diagonal compared to smaller capillary numbers: compare Fig. 8(a) with Fig. 8(b). For the higher capillary number, s_{ij} and r_{ij} are only weakly correlated.

Last, we check Eq. (25) in Sec. IV D in Fig. 9. That is, we plot $-\langle q_{ij}(\Delta p_{ij} - p_{c,ij})\rangle$ and $\langle |q_{ij}|\rangle\langle |(\Delta p_{ij} - p_{c,ij})|\rangle$ as a function of the saturation s. The prediction of Eq. (25) is that the two quantities should be the equal. For both capillary numbers this works well.

VI. CONCLUSION AND PERSPECTIVE

We have presented a statistical mechanical analysis of immiscible two-phase flow in porous media through the introduction and analysis of the ensemble distribution $\Pi(x_{b,ij}, s_{ij}, r_{0,ij})$ which gives the joint probability density between center-of-mass position of the bubbles, the saturation, and the radius of any link in the network that models the porous medium. With the ensemble distribution, any quantity that does not require the relative positions of the links to be taken into account may be calculated. We have presented a few examples in Sec. IV, among them the fractional flow, the average saturation, the average pressure difference leading to the effective mobility, and finally the entropy production or dissipation. Questions that cannot be answered within this approach are, e.g., the relative statistical weight of a given configuration of interfaces within the system which, e.g., comes up in connection with the construction of the Markov-chain Monte Carlo method for sampling fluid configurations. For such questions, the configurational probability density is necessary [30].

The ensemble distribution $\Pi(x_{b,ij}, s_{ij}, r_{0,ij})$ introduced here relates the dynamics of the system to a probability distribution that does not contain time. This is possible due to the ergodicity of the system; see Sec. III. However, since the probability distribution does not contain time, it cannot answer questions that have to do with time explicitly; e.g., questions concerning correlation time is outside the realm of this approach.

The ensemble distribution may be transformed into the link volume flow distribution $\Pi_q(|q_{ij}|, s_{ij}, r_{0,ij})$. This has a surprisingly simple form for moderate capillary numbers; see Eq. (28). This probability distribution is a close relative of the current distribution function in the random resistor network that was extensively studied and shown to be multifractal in the 1980s [52,53]. We expect to find similar complications in the present system when the saturation is at the critical point studied by Ramstad *et al.* [51].

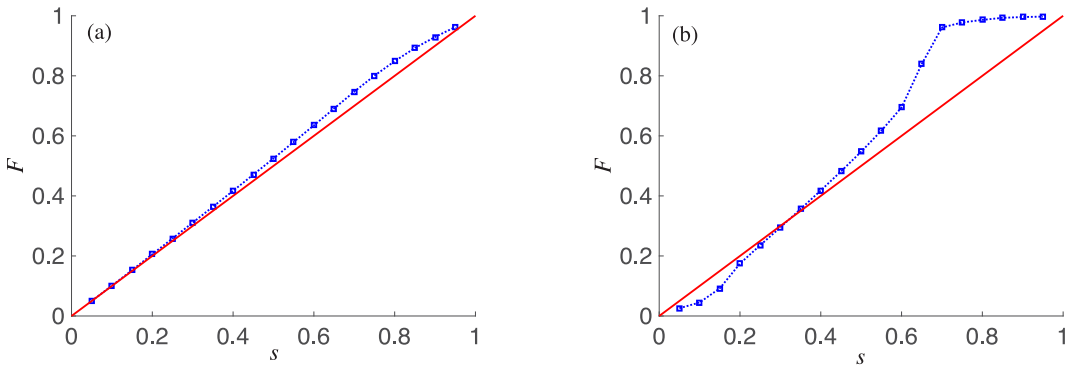

FIG. 8. The nonwetting fractional flow defined in Eq. (17) F vs the volume averaged saturation s defined in Eq. (18) for (a) Ca $= 0.1$ and (b) Ca $= 0.01$.

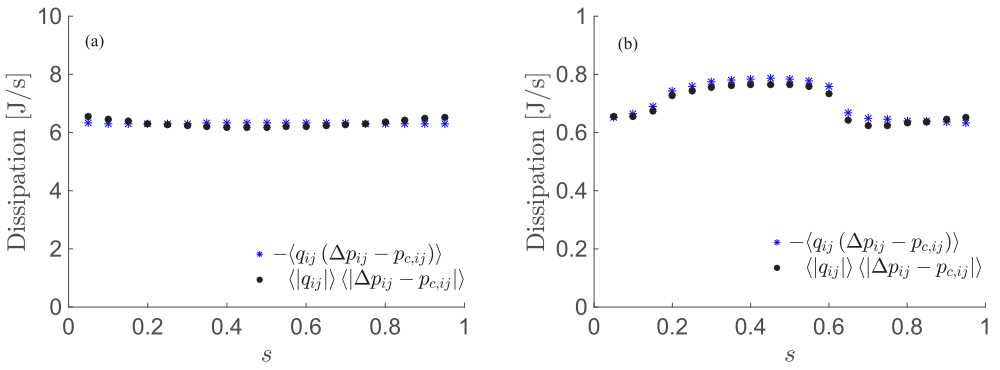

FIG. 9. The dissipation $-\langle q_{ij}(\Delta p_{ij} - p_{c,ij})\rangle$ and $\langle |q|\rangle\langle |\Delta p - p_{c,ij}|\rangle$ plotted against the nonwetting saturation for (a) Ca = 0.1 and (b) Ca = 0.01. Equation (25) predicts that the two data sets should be equal. The system size was 20×20.

ACKNOWLEDGMENTS

I.S., S.K., and A.H. thank VISTA, a collaboration program between Statoil and the Norwegian Academy of Science and Letters, for financial support. M.V. thanks the NTNU for financial support. S.S. thanks the Research Council of Norway (RCN) and the Beijing Computational Science Research Center (CSRC) for financial support. The numerical calculations were made possible through a grant of computer time by NOTUR, the Norwegian Metacenter for Computational Science.

APPENDIX: NETWORK MODEL

We use the network model shown in Fig. 1 [27,28] to test some of the central ideas presented in this work. The links represent cylindrical tubes of varying average radii, containing the volume of both the pores and the pore throats of the porous medium. Each link is hourglass shaped so that the capillary pressure due to an interface at position $0 \leqslant x \leqslant l$ in the link is given by

$$|p_{c,ij}(x)| = \frac{2\gamma\cos\theta}{r_0}\left[1 - \cos\left(\frac{2\pi x}{l}\right)\right], \tag{A1}$$

where γ is the surface tension. The volume flow in each link is related to the pressure difference across it by the Washburn equation

$$q_{ij} = -\frac{\pi r_{0,ij}^4}{8\mu_{av,ij}}(\Delta p_{ij} - p_{c,ij}), \tag{A2}$$

where Δp_{ij} is the pressure difference across the link and $p_{c,ij}$ is the sum of the capillary pressure contribution from all the interfaces in the link. For a link with a single bubble with center-of-mass position $x_{b,ij}$ and saturation s_{ij}, and surface tension γ, the capillary pressure on the bubble is given by [46]

$$p_{c,ij}(x_{b,ij}, s_{ij}, r_{0,ij}) = \frac{4\gamma}{r_{0,ij}}\sin(\pi s_{ij})\sin\left(\frac{2\pi x_{b,ij}}{l}\right). \tag{A3}$$

At each node volume flow is conserved. This implies that the sum of the contributions from Eq. (A2) are conserved at the nodes. This results in a matrix equation for the pressure field. After solving this equation we can use Eq. (A2) to calculate the flow in each link. From the flow, we can calculate the velocity $u_{ij} = q_{ij}/\pi r_{0,ij}^2$ of the fluids. We then move every bubble an amount $\Delta x_{ij} = u_{ij}\Delta t$, where the time step Δt is chosen such that no bubble moves more than 10% of the link length.

When the fluid reaches the end of a link, it is redistributed into connected links in proportion to the local flow. If at any given point there are more than three bubbles present in a link, the closest two are merged such that the center of mass of the merged bubbles is conserved. Further details can be found in Refs. [27,28].

[1] J. Bear, *Dynamics of Fluids in Porous Media* (Dover, Mineola, NY, 1988).
[2] R. D. Wyckoff and H. G. Botset, Physics **7**, 325 (1936).
[3] J. S. Osoba, J. G. Richardson, J. K. Kerver, J. A. Hafford, and P. M. Blair, J. Petroleum Techology **3**, 47 (1951).
[4] R. G. Larson, L. E. Scriven, and H. T. Davis, Chem. Eng. Sci. **36**, 57 (1981).
[5] W. G. Gray, Int. J. Multiphase Flow **15**, 81 (1989).
[6] S. M. Hassanizadeh and W. G. Gray, Adv. Water Resour. **13**, 169 (1990).
[7] S. M. Hassanizadeh and W. G. Gray, Adv. Water Resour. **16**, 53 (1993).
[8] S. M. Hassanizadeh and W. G. Gray, Water Resour. Res. **29**, 3389 (1993).
[9] W. G. Gray and S. M. Hassanizadeh, Adv. Water Resour. **21**, 261 (1998).
[10] R. Hilfer, Phys. Rev. E **58**, 2090 (1998).
[11] W. G. Gray, Adv. Water Resour. **22**, 521 (1999).
[12] R. Hilfer and H. Besserer, Physica B **279**, 125 (2000).
[13] R. Hilfer, Physica A **359**, 119 (2006).

[14] R. Hilfer, Phys. Rev. E **73**, 016307 (2006).
[15] R. Hilfer, Physica A **371**, 209 (2006).
[16] A. Hansen and T. Ramstad, Comput. Geosci. **13**, 227 (2009).
[17] R. Hilfer and F. Döster, Transp. Porous Media **82**, 507 (2010).
[18] J. Niessner, S. Berg, and S. M. Hassanizadeh, Transp. Porous Media **88**, 133 (2011).
[19] F. Döster, O. Hönig, and R. Hilfer, Phys. Rev. E **86**, 016317 (2012).
[20] R. Hilfer, R. T. Armstrong, S. Berg, A. Georgiadis, and H. Ott, Phys. Rev. E **92**, 063023 (2015).
[21] S. M. Hassanizadeh, in *Handbook of Porous Media*, 3rd ed., edited by K. Vafai (CRC Press, Boca Raton, FL, 2015).
[22] M. S. Valavanides and T. Daras, Entropy **18**, 54 (2016).
[23] B. Ghanbarian, M. Sahimi, and H. Daigle, Water Resour. Res. **52**, 5025 (2016).
[24] A. Hansen, S. Sinha, D. Bedeaux, S. Kjelstrup, I. Savani, and M. Vassvik, arXiv:1605.02874.
[25] M. J. Blunt, B. Bijeljic, H. Dong, H. Gharbi, S. Iglauer, P. Mostaghimi, A. Paluzny, and C. Pentland, Adv. Water Resour. **51**, 197 (2013).
[26] S. Bryant and M. J. Blunt, Phys. Rev. A **46**, 2004 (1992).
[27] E. Aker, K. J. Måløy, A. Hansen, and G. G. Batrouni, Transp. Porous Media **32**, 163 (1998).
[28] H. A. Knudsen, E. Aker, and A. Hansen, Transp. Porous Media **47**, 99 (2002).
[29] G. Tørå, P. E. Øren, and A. Hansen, Transp. Porous Media **92**, 145 (2012).
[30] I. Savani, S. Sinha, D. Bedeaux, S. Kjelstrup, and M. Vassvik, Transp. Porous Media **116**, 869 (2017).
[31] V. Joekar-Niasar and S. M. Hassanizadeh, Crit. Rev. Environ. Sci. Technol. **42**, 1895 (2012).
[32] T. Ramstad, P. E. Øren, and S. Bakke, SPEJ, Soc. Pet. Eng. J. **15**, 917 (2010).
[33] T. Ramstad, N. Idowu, C. Nardi, and P. E. Øren, Transp. Porous Media **94**, 487 (2012).
[34] S. Berg, M. Rücker, H. Ott, A. Georgiadis, H. van der Linde, F. Ensmann, M. Kersten, R. T. Armstrong, S. de With, J. Becker, and A. Wiegmann, Adv. Water Resour. **90**, 24 (2016).
[35] R. T. Armstrong, J. E. McClure, M. A. Berrill, M. Rücker, S. Schlüter, and S. Berg, Phys. Rev. E **94**, 043113 (2016).
[36] A. M. Tartakovsky and P. Meakin, J. Comput. Phys. **207**, 610 (2005).
[37] S. Ovaysi and M. Piri, J. Comput. Phys. **229**, 7456 (2010).
[38] M. B. Liu and G. R. Liu, Arch. Comput. Methods Eng. **17**, 25 (2010).
[39] R. T. Armstrong, S. Berg, O. Dinariev, N. Evseev, D. Klemin, D. Koroteev, and S. Safanov, Transp. Porous Media **112**, 577 (2016).
[40] S. Kjelstrup and D. Bedeaux, *Non-Equilibrium Thermodynamics of Heterogeneous Systems* (World Scientific, Singapore, 2008).
[41] S. Kjelstrup, D. Bedeaux, E. Johannesen, and J. Gross, *Non-Equilibrium Thermodynamics for Engineers* (World Scientific, Singapore, 2010).
[42] E. C. Childs and N. Collis-George, Proc. R. Soc. London **201**, 392 (1950).
[43] A. E. Scheidegger, J. Appl. Phys. **25**, 994 (1954).
[44] A. E. Scheidegger, Trans. Soc. Rheol. **9**, 313 (1965).
[45] R. H. Aranow, Phys. Fluids **9**, 1721 (1966).
[46] S. Sinha, A. Hansen, D. Bedeaux, and S. Kjelstrup, Phys. Rev. E **87**, 025001 (2013).
[47] S. Bakke and P. E. Øren, SPEJ, Soc. Pet. Eng. J. **2**, 136 (1997).
[48] M. Sahimi, *Flow and Transport in Porous Media and Fractured Rock*, 2nd ed. (Wiley-VCH, Weinheim, 2011).
[49] M. Erpelding, S. Sinha, K. T. Tallakstad, A. Hansen, E. G. Flekkøy, and K. J. Måløy, Phys. Rev. E **88**, 053004 (2013).
[50] G. G. Batrouni, A. Hansen, and M. Nelkin, J. Phys. **48**, 771 (1987).
[51] T. Ramstad, A. Hansen, and P. E. Øren, Phys. Rev. E **79**, 036310 (2009).
[52] L. de Arcangelis, S. Redner, and A. Coniglio, Phys. Rev. B **31**, 4725 (1985).
[53] G. G. Batrouni, A. Hansen, and B. Larson, Phys. Rev. E **53**, 2292 (1996).
[54] L. Zhu, N. Jin, Z. Gao, and Y. Zong, Pet. Sci. **11**, 111 (2014).